

Analysis of atmospheric pressure and temperature effects on cosmic ray measurements

R. R. S. De Mendonça,¹ J. -P. Raulin,² E. Echer,¹ V. S. Makhmutov,³ and G. Fernandez⁴

Received 12 June 2012; revised 28 September 2012; accepted 17 November 2012; published 30 April 2013.

[1] In this paper, we analyze atmospheric pressure and temperature effects on the records of the cosmic ray detector CARPET. This detector has monitored secondary cosmic ray intensity since 2006 at Complejo Astronómico El Leoncito (San Juan, Argentina, 31°S, 69°W, 2550 m over sea level) where the geomagnetic rigidity cutoff, R_c , is ~ 9.8 GV. From the correlation between atmospheric pressure deviations and relative cosmic ray variations, we obtain a barometric coefficient of -0.44 ± 0.01 %/hPa. Once the data are corrected for atmospheric pressure, they are used to analyze temperature effects using four methods. Three methods are based on the surface temperature and the temperature at the altitude of maximum production of secondary cosmic rays. The fourth method, the integral method, takes into account the temperature height profile between 14 and 111 km above Complejo Astronómico El Leoncito. The results obtained from these four methods are compared on different time scales from seasonal time variations to scales related to the solar activity cycle. Our conclusion is that the integral method leads to better results to remove the temperature effect of the cosmic ray intensity observed at ground level.

Citation: De Mendonça, R. R. S., J. -P. Raulin, E. Echer, V. S. Makhmutov, and G. Fernandez (2013), Analysis of atmospheric pressure and temperature effects on cosmic ray measurements, *J. Geophys. Res. Space Physics*, 118, 1403–1409, doi:10.1029/2012JA018026.

1. Introduction

[2] Investigations of the physical nature of the cosmic ray variations in different time scales are an important subject in cosmic ray physics and astrophysics. More specifically, the modulation of cosmic rays is an important tool to describe disturbed conditions in the heliosphere. Longer time scales are related to the solar activity cycle, while faster variations of the order of minutes to hours and days, can be associated with solar transient events, geomagnetic disturbances, and Earth's atmospheric phenomena.

[3] When analyzing variations in cosmic ray intensity using ground-based detectors, atmospheric effects on the flux of secondary particles cannot be ignored. The pressure and temperature effects produce significant background variations. Thus, it is important to remove these effects from

ground-based data, before studying its relation with any extraterrestrial phenomena [Dorman, 2004].

[4] The pressure effect on secondary cosmic ray variations has been known for a long time. Myssowsky and Tuwim [1926] and Steinke [1929] are among the first who have studied the relation between cosmic ray time variations and atmospheric pressure changes. The barometric effect is experimentally determined by equation (1):

$$\left(\frac{\Delta I}{I}\right)_P = \beta \cdot \Delta P \quad (1)$$

where $(\Delta I/I)_P$ is the normalized deviation of the cosmic ray intensity related with the pressure effect, ΔP is the atmospheric pressure deviation and β is the barometric coefficient, which depends on many factors, such as the nature of the secondary component and the altitude where the observation is performed [Dorman, 2004]. Atmospheric temperature change is an additional cause for the seasonal/annual variations of cosmic ray intensities detected by ground-based instruments. The seasonal modulation has its maximum and minimum in winter and summer, respectively. Generally, the temperature effect is described in two different ways, called negative and positive temperature effects [Dorman, 2004, and references therein]. The negative effect corresponds to the decrease of muon intensity at ground level, since more muons decay during the heating and the expansion of the atmosphere from winter to summer due to the increase of their propagation path [Blackett, 1938]. The positive effect is related to the temperature influence on muon production from the decay of charged pions [Duperier, 1949].

¹National Institute for Space Research, Division of Space Geophysics, Av. dos Astronautas, Jd. Granja, Sao Jose dos Campos SP, Brazil.

²Centro de Rádio Astronomia e Astrofísica Mackenzie, EE, UPM, Rua da Consolacao, 896 - Edifício Reverendo Modesto Carvalhosa, 7° andar, Consolacao, Sao Paulo, SP, Brazil.

³Lebedev Physical Institute of the Russian Academy of Sciences (Solar and Cosmic Ray Physics Laboratory), Moscow, Russia.

⁴Complejo Astronómico el Leoncito, CONICET, San Juan, Argentina.

Corresponding author: R. R. S. De Mendonça, National Institute for Space Research - INPE, Division of Space Geophysics, Av. dos Astronautas, 1758, Jd. Granja, 12227-010, São José dos Campos, SP, Brazil. (mendonca@dge.inpe.br)

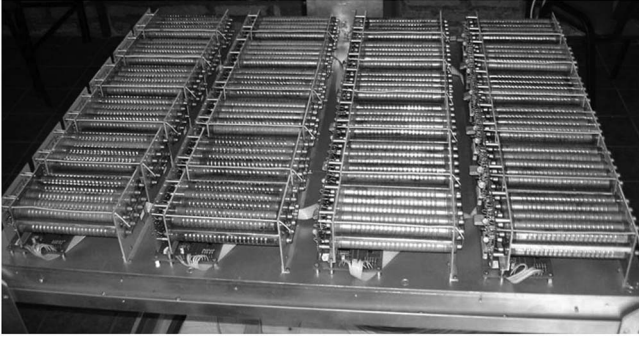


Figure 1. The CARPET cosmic ray detector.

[5] In general, experimental studies of the temperature effect on secondary cosmic ray intensity consider one or more terms on the right-hand side of the following equation [Dorman, 2004]:

$$\left(\frac{\Delta I}{I}\right)_T = K_G \Delta T(h_G) + C_H \Delta H(h_M) + K_M \Delta T(h_M) \quad (2)$$

where $(\Delta I/I)_T$ is the normalized deviation of the cosmic ray intensity related with the temperature effect, $\Delta T(h_G)$ is the ground temperature deviation, $\Delta H(h_M)$ and $\Delta T(h_M)$ are respectively the height deviation and the temperature deviation at the altitude of maximum production of secondary particles. Wang and Lee [1967] is an example of a study that uses the two last terms of the equation (1). Duperier [1949], Trefall [1957], Hayakawa et al. [1955], French and Chasson [1959] and Mathews [1959] are examples of studies that use the second and/or the third term of the equation (2). Studies using the first term were more common before 1950, e.g., Hess [1940].

[6] There is also an approach to describe the temperature effect, which is called the integral method [Maeda and Wada, 1954; Dorman, 1972; Sagisaka, 1986]. Differently from the methods shown above, the integral method takes into account the temperature along the whole vertical atmospheric path rather than at a single altitude range. Thus, the temperature effect is given by the following relation:

$$\left(\frac{\Delta I}{I}\right)_T = \int_0^p \alpha(x) \Delta T(x) dx \quad (3)$$

where $(\Delta I/I)_T$ is the normalized deviation of the cosmic ray intensity related with the temperature effect at the atmospheric pressure p , $\Delta T(x)$ is the temperature deviation for this atmospheric pressure x , $\alpha(x)$ is the temperature coefficient at this same atmospheric pressure. This method or its variations were used by Ambrosio et al. [1997], Yanchukovsky et al. [2007], Berkova et al. [2008], Adamson et al. [2010], and Berkova et al. [2011].

[7] In this paper, we compare cosmic ray time variations observed by CARPET detector with atmospheric pressure and temperature changes. First we calculate the barometric coefficient and we obtain the pressure corrected CARPET cosmic ray data. Then, in order to analyze and correct for the temperature effect, we propose and compare four different methods: (I) considering the ground temperature variations, i.e., the first term in equation (2); (II) considering the

temperature variations at the altitude of maximum secondary cosmic ray production, i.e., the third term in equation (2); (III) considering both the first and the third terms in equation (2); and (IV) considering an approximation of the integral method. For the last method, differently to what has been done before, we have used experimental data to calculate both $\alpha(x)$ and $\Delta T(x)$. We mention that this method assumes that each atmospheric layer behaves independently from one of the others in response to temperature variations. This may not be totally correct, and therefore indicates the limitations of our integral method.

2. Instrumentation

[8] This study is based on the cosmic ray intensity data provided by the CARPET detector shown in Figure 1, and temperature records measured at ground level and between 14 and 111 km of altitude. The CARPET detector was installed in April 2006 at CASLEO (Complejo Astronómico El Leoncito), San Juan, Argentina, (31°S , 69°W , $R_c = 9.8$ GV, 2550 m of altitude). This detector was designed and developed by the Lebedev Physical Institute (LPI, Moscow, Russia) within an international scientific cooperation between the LPI, the CRAAM (Centro de Rádio Astronomia e Astrofísica Mackenzie, São Paulo, Brazil) and CASLEO.

[9] As shown in Figure 1, the CARPET consists of 24 blocks of 10 gas-discharge cylindrical STS-6 Geiger counters, located on a platform of $\sim 1.5 \times 1.5$ m in size. Each counter has a diameter of ~ 2 cm and length of ~ 10 cm. Each block consists of five upper and five lower counters, separated by an aluminum absorber with a thickness of 7 mm. The electronics of the instrument allows to record three channels data with a time resolution in the range from 250 ms to 10 s. In this paper we use an integration time of 500 ms. We only use the data from the channel N12, which corresponds to the total counts recorded in coincidence between upper and lower tubes of each block. This channel mainly detects electrons with $E > 5$ MeV, protons with $E > 30$ MeV, and muons with $E > 20$ MeV.

[10] The ground temperature data are provided by a meteorological station installed near the CARPET detector. It measures the ground temperature value every 30 min. The temperature height profiles observed between 14 and 111 km are provided by the SABER (Sounding of the Atmosphere Using Broadband Emission Radiometry) instrument on NASA's Thermosphere, Ionosphere, Mesosphere, Energetics and Dynamics mission, see more details about SABER at <http://saber.gats-inc.com>. We have selected the temperature height profiles above CASLEO's location (area within 20°S – 40°S , 60°W – 80°W). In general, over this region, more than one measurement per day is made, so the SABER's data are processed to get a daily mean temperature profile with a resolution of 0.5 km. No SABER temperature data measurements are available below 14 km.

3. Analysis, Results and Discussions

3.1. Pressure Effect

[11] The atmospheric pressure analysis was made using the hourly data observed on July 2009. During this period there were no significant geomagnetic and solar disturbances. No large variations of the ground temperature were

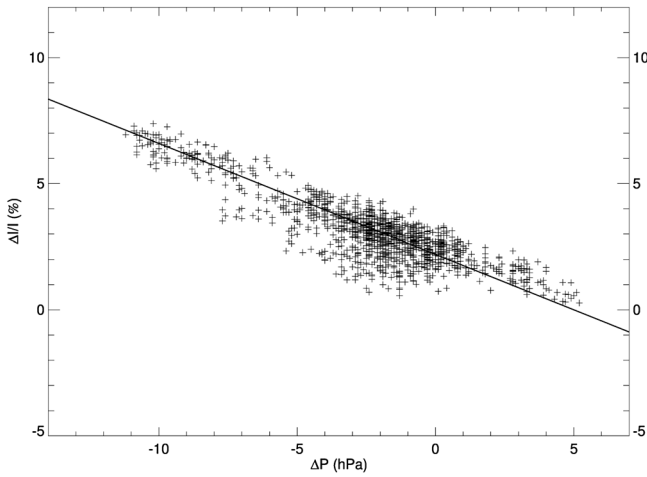


Figure 2. The anticorrelation between the pressure deviation and the relative cosmic ray intensity variation observed by the channel N12 of CARPET detector on July 2009. The black continuous line is given by $Y = 2.2 - 0.44 * X$ and the correlation coefficient is 0.9.

observed. Finally, during this period we have also verified that there was no atmospheric electric field variations nor rain occurrence (see *De Mendonça et al.* [2011] for details of the influence of atmospheric electric field variations and rain occurrence on the cosmic ray intensity observed by the CARPET detector). We have analyzed the atmospheric pressure deviation (ΔP) and the corresponding relative deviation of the cosmic ray intensity ($\Delta I/I$) observed by the

channel N12. Figure 2 shows the correlation found between $\Delta I/I$ and ΔP . Using a least-squares fitting method, we found the barometric coefficient $\beta \sim -0.44 \pm 0.01$ %/hPa and a correlation coefficient ~ 0.9 . Figure 3 shows an example of the pressure correction by comparing uncorrected (top panel), and corrected (bottom panel) cosmic ray records, with pressure time variations (middle panel). An increase of the uncorrected cosmic ray intensity occurred between 20 and 24 March 2010, which was clearly related with a decrease of the atmospheric pressure during the same period. This variation practically disappears in the pressure corrected data. It is believed that the small amplitude of the diurnal variation that occurs in this period is associated with interplanetary phenomena.

3.2. Temperature Effect

[12] The database used for the temperature analysis is composed by the cosmic ray intensities corrected for pressure effects, $(\Delta I/I)_{PC}$, and temperature height profiles measured between April 2006 and August 2010. The temperature data were processed to get $\Delta T(h)$, which corresponds to the temperature deviation at a given altitude h .

[13] In the first method, as illustrated in Figure 4A, a clear anticorrelation can be observed between $(\Delta I/I)_{PC}$ and $\Delta T(h_G)$, where $h_G = 2550$ m is the altitude of CASLEO. The ground temperature coefficient (K_G) obtained from the anticorrelation shown in Figure 4B, is: -0.40 ± 0.02 %/°C, and the correlation coefficient is 0.81.

[14] Figure 5A illustrates the second method and compares $(\Delta I/I)_{PC}$ with the temperature deviations at the altitude of the maximum production of secondary cosmic rays ΔT

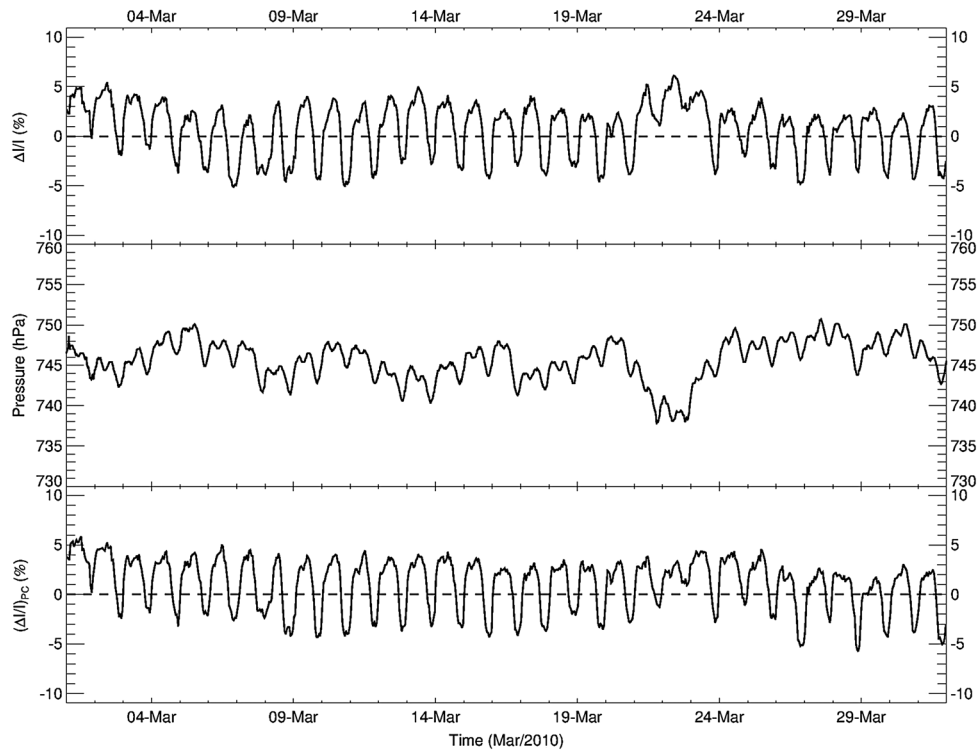


Figure 3. (top) The uncorrected cosmic ray data, (middle) the atmospheric pressure, and (bottom) the pressure corrected cosmic ray data observed between 1 March 2010 and 1 April 2010. All data are presented in hourly mean values.

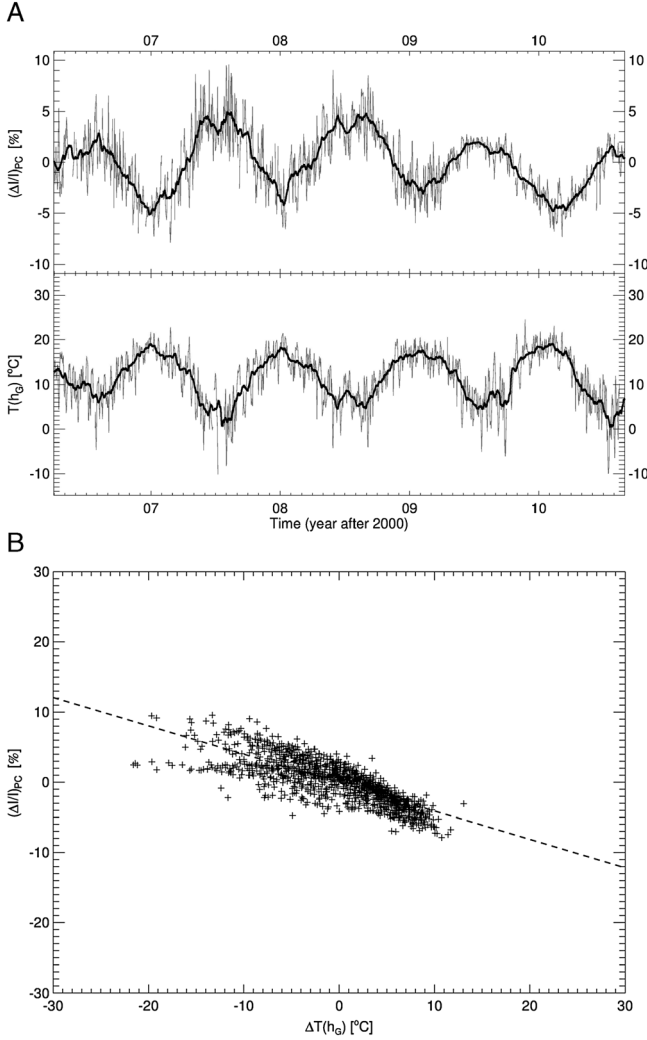


Figure 4. (A) Monthly (black curve) and daily (grey curve) means of pressure corrected cosmic ray data $(\Delta I/I)_{PC}$ and of the ground temperature $T(h_G)$ observed between April 2006 and August 2010 at CASLEO. (B) The anticorrelation obtained between the ground temperature deviation $\Delta T(h_G)$ and the relative variation of the pressure corrected cosmic ray intensity $(\Delta I/I)_{PC}$ both calculated using the data shown in Figure 4A. The dashed line is given by $Y=0.41 - 0.40 \cdot X$ and the correlation coefficient is 0.81.

($h_M = 16$ km). When comparing these two parameters it is possible to observe a rough positive correlation between them. The correlation coefficient (see Figure 5B) obtained in this case (0.54) is lower than that obtained analyzing $(\Delta I/I)_{PC}$ and $\Delta T(h_G)$. Thus, the anticorrelation between $(\Delta I/I)_{PC}$ and $\Delta T(h_G)$ is more significant than the correlation obtained using $\Delta T(h_M)$. The temperature coefficient (K_M) at the altitude h_M obtained by the correlation shown in Figure 5B is 0.67 ± 0.09 %/°C.

[15] Positive values of K_M indicate that the temperature effect at 16 km of altitude is more likely related to the temperature influence on pion decay (the positive temperature effect). By contrast, the negative values of K_G are related to the negative temperature effect (muon intensity decrease related to expansion of the atmosphere).

[16] In order to get rid of the temperature effect from the cosmic ray data, we assume that the relative cosmic ray intensity measured and corrected for pressure $(\Delta I/I)_{PC}$ has two components: one associated with temperature variations, called $(\Delta I/I)_T$, and one free from temperature variations. Thus, the relative cosmic ray data corrected for the temperature and pressure effects $(\Delta I/I)_{TPC}$ is given by:

$$\left(\frac{\Delta I}{I}\right)_{TPC} = \left(\frac{\Delta I}{I}\right)_{PC} - \left(\frac{\Delta I}{I}\right)_T \quad (4)$$

[17] The first and second panels from the top in Figure 6 show $(\Delta I/I)_{PC}$ and $(\Delta I/I)_{TPC}$ obtained using the first and second method where we assume that $(\Delta I/I)_T = K_G \cdot \Delta T(h_G)$ and

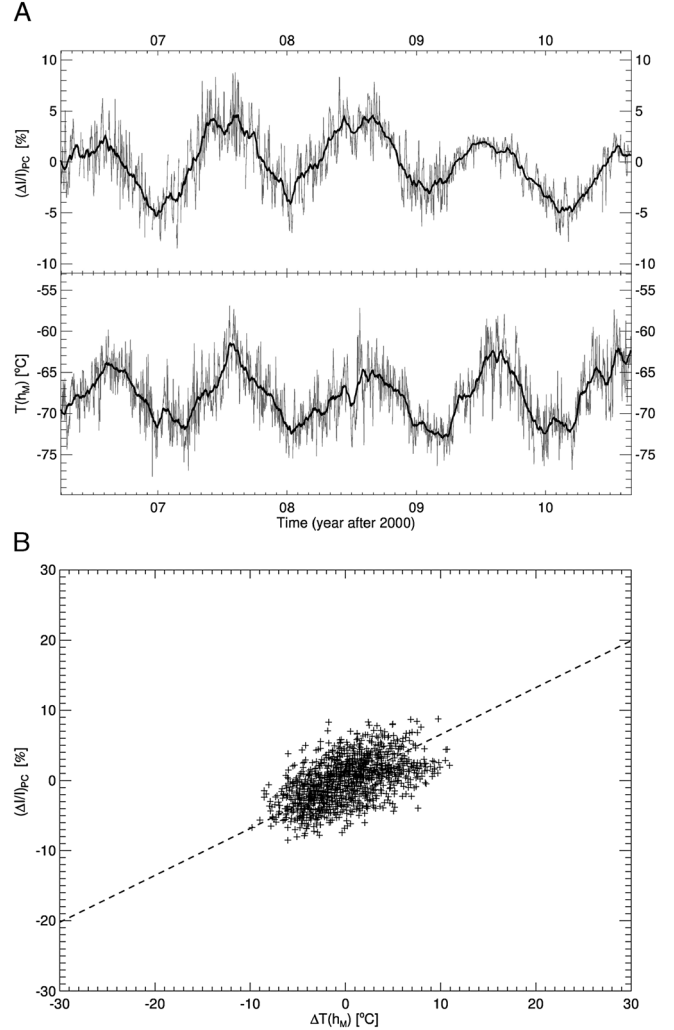


Figure 5. (A) Monthly (black curve) and daily (grey curve) means of pressure corrected cosmic ray data $(\Delta I/I)_{PC}$ and of the temperature at altitude of maximum secondary cosmic ray production $T(h_M)$ observed between April 2006 and August 2010 at CASLEO. (B) The anticorrelation obtained between the deviation of the temperature at altitude of maximum secondary cosmic ray production $\Delta T(h_M)$ and the relative variation of the pressure corrected cosmic ray intensity $(\Delta I/I)_{PC}$ both calculated using the data shown in Figure 5A. The dashed line is given by $Y=-0.14 + 0.67 \cdot X$ and the correlation coefficient is 0.54.

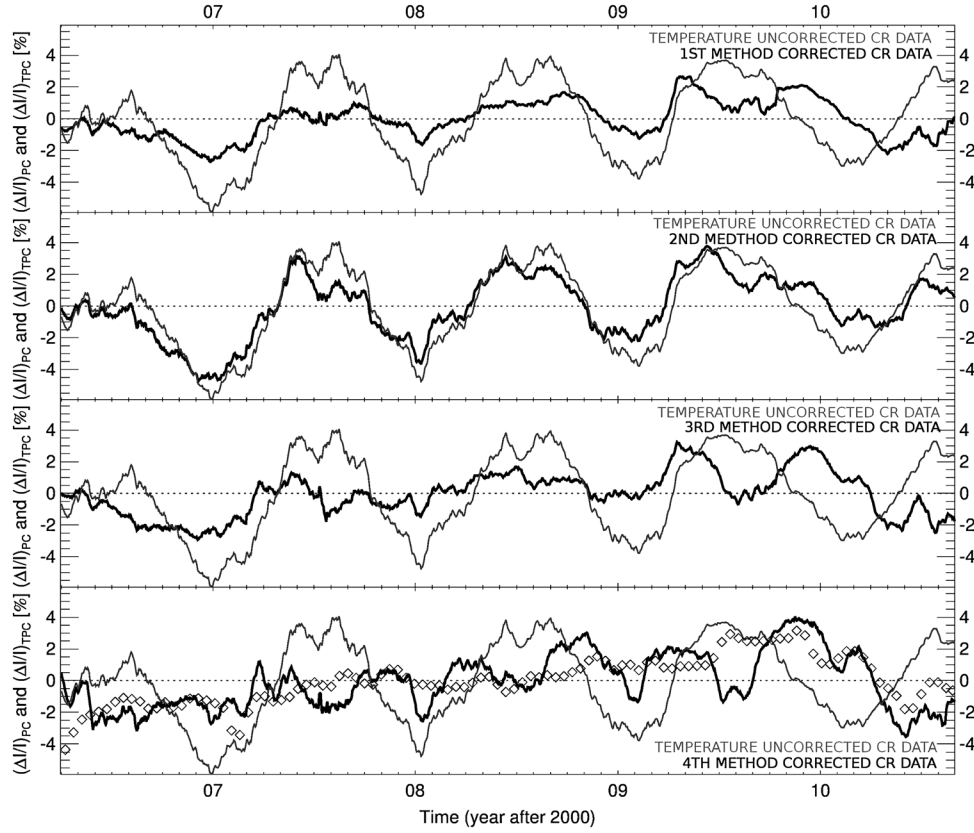


Figure 6. Monthly mean values of uncorrected by temperature cosmic ray intensity and of first, second, third, and fourth temperature methods corrected cosmic ray intensity observed by the CARPET detector between April 2006 and August 2010. The diamonds in the last panel represent the cosmic ray variation observed by the Moscow Neutron Monitor.

$(\Delta I/I)_T = K_M \cdot \Delta T(h_M)$, respectively. We note that the data corrected by the first method present a significant reduction of the amplitude of the seasonal variation, contrary to the data corrected by the second method. This is probably related to the rough positive correlation between $(\Delta I/I)_{PC}$ and $\Delta T(h_M)$.

[18] When the third method is applied, the cosmic ray data are first corrected considering $\Delta T(h_M)$ and $\Delta T(h_G)$. As a first step the cosmic ray data are corrected similarly to the second method (using the values of K_M already shown). After, they are corrected similarly to the first method, using a new value of the ground temperature coefficient. This new coefficient is calculated through the correlation between the second method corrected cosmic ray data and ground temperature variation. As it is possible to see in the third panel from the top of Figure 6, the resulting corrected data using this method do not differ from the data corrected using the first method. This result does not change when the cosmic ray data are first corrected using the first method and then corrected using the second method.

[19] As for the fourth method, and due to data limitations, an approximation of the integral method shown in the equation (3) is used:

$$\left(\frac{\Delta I}{I}\right)_T = \sum_{h_1}^{h_F} \alpha(h) \cdot \Delta T(h) + \alpha_G \cdot \Delta T(h_G) \quad (5)$$

where $\Delta T(h)$ is the temperature deviation at a given altitude h , $\alpha(h)$ is the temperature coefficient for this altitude, h_1 is

the altitude where the atmospheric depth is close to zero ($h_1 = 111.0$ km), h_F is equal to 14.0 km, $\Delta T(h_G)$ is the ground temperature deviation ($h_G = 2.5$ km), and α_G is the temperature coefficient at ground level.

[20] We obtained a value of $\alpha(h)$ for each layer separated by 0.5 km step between 14 and 111 km. These coefficients are

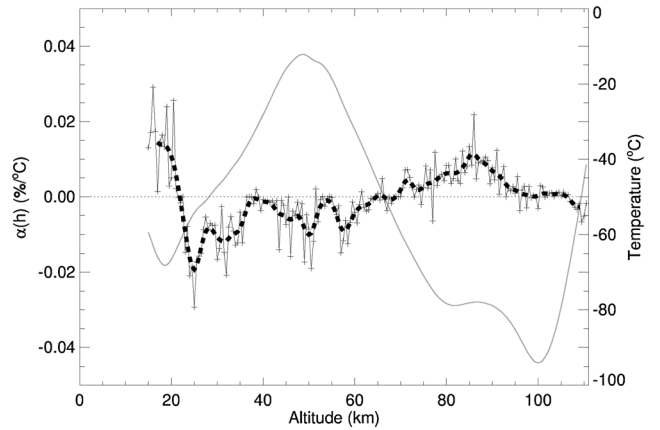


Figure 7. The continuous curve with crosses represents $\alpha(h)$ values obtained. The black dashed curve represents the smoothing of these values and the continuous grey curve represents the typical temperature altitude profile observed by the SABER instrument.

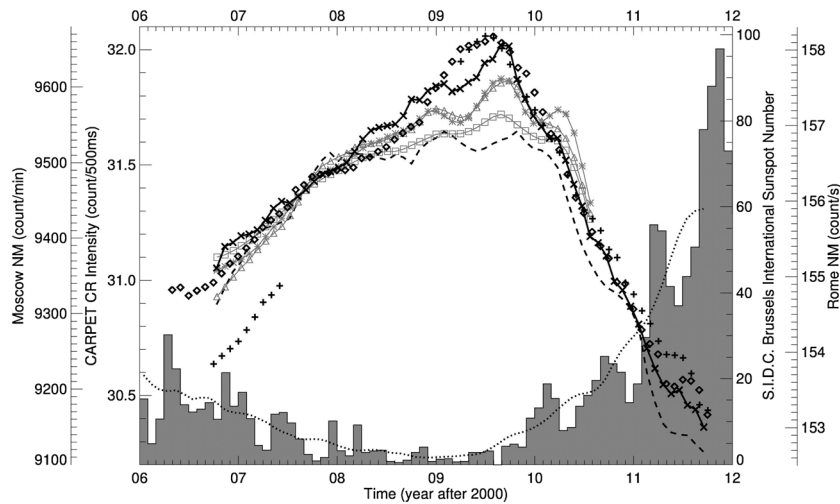


Figure 8. The Moscow and Rome Neutron Monitors measurements (diamonds and plus symbols respectively). The CARPET temperature uncorrected cosmic ray data (dashed black curve) and the corrected data using: first method (grey curve with squares), second method (grey curve with triangles), and third method (grey curve with asterisks) observed between 2006 and 2010. The black curve with crosses shows the fourth method corrected cosmic ray data and the grey histograms and black dotted curve shows the monthly mean and 13 months smoothed Brussels Sunspot Number. The bar in the left upper corner indicates the upper limit of the RMS estimated on daily mean data.

calculated as follows: $\alpha(111 \text{ km})$ is first computed by comparing $(\Delta/I)_{PC}$ and $\Delta T(111 \text{ km})$ measured between April 2006 and August 2010, and used to correct our cosmic ray data. These corrected data are then used to estimate $\alpha(110.5 \text{ km})$. This procedure is repeated in an iterative way to get $\alpha(14.0 \text{ km})$. Finally, α_G is calculated comparing the final corrected cosmic ray data and $\Delta T(h_G)$. The results are shown in Figure 7 where we compare $\alpha(h)$ and temperature as a function of height. Note that near the altitude h_M the values of $\alpha(h)$ are positive, in agreement with the analysis made using the second method. Moreover, on the ground altitude $\alpha(h_G) = -0.09 \pm 0.02 \text{ \%}^\circ\text{C}$ is negative, which is in agreement with the analysis made using the first method. However, the values of $\alpha(h_M)$ and $\alpha(h_G)$ are smaller than the values of K_M and K_G .

[21] In order to verify our correction of cosmic ray flux for temperature variations, we have applied the same method to the period between July 2009 and December 2010 during which atmospheric pressure remains almost constant at CASLEO ($P_{\text{mean}} = 744 \pm 3 \text{ hPa}$). As a result we have found the same correction coefficients to within 9%, confirming the relevance of the method. Finally, a preliminary comparison between the temperature coefficients obtained in this paper and the ones obtained considering the atmospheric layers not independent suggests that they are in good agreement [Yanke *et al.*, 2011].

[22] The comparison of the results obtained by the different methods and with the uncorrected data is shown in Figure 6. On longer time scales related to the solar activity cycle, we note also significant differences between the uncorrected and the corrected data. This is illustrated in Figure 8, where cosmic ray data are compared with the S.I.D.C. Brussels International Sunspot Number [http://www.swpc.noaa.gov]. Between November 2007 and April 2010, the uncorrected data present a very flat intensity maximum, while the corrected data tend to present a more defined peak. The data

corrected using the integral method present the best defined peak, which occurs close to the period when the sunspot number presents its lower values. This peak-shaped cosmic ray maximum during the last solar minimum is expected due to the well known 22 year cosmic ray cycle [Webber and Lockwood, 1988]. We also note a decrease of the cosmic ray intensity after April 2010 associated with an increasing solar activity during the same period.

4. Conclusions

[23] In this work we have analyzed and corrected the cosmic ray data from CARPET detector for atmospheric pressure effect. We also use four different methods to describe and correct for the temperature effect.

[24] We analyzed the cosmic ray and atmospheric pressure data measured on July 2009, when significant variations of the atmospheric pressure were observed without significant influences from solar and geophysical phenomena. From this analysis, we obtain a barometric coefficient equal to $-0.44 \pm 0.01 \text{ \%}/\text{hPa}$.

[25] In the analysis of the temperature effect, we found an anticorrelation between the relative variations of the cosmic ray intensity and the surface temperatures. Moreover, a correlation was found between relative variations of the cosmic ray data and the temperature at the altitude of maximum production of secondary particles. The cosmic ray data corrected by the first method presented a large reduction of the seasonal variation, while the data corrected by the temperature at the altitude h_M presented a small reduction. The results obtained using the third method do not differ from those obtained using the first method. Data corrected using the fourth method removed most of the seasonal variations. Moreover, the cosmic ray intensities corrected by the fourth method have shown peak-shaped maximum values in August to September 2009 well associated with the 23rd solar

activity minimum. Thus, the fourth correction method, or integral method, is believed to be the most suitable among the others due to the best removal temperature effects superimposed on the seasonal variation and the good anticorrelation with the solar activity cycle between 2006 and 2012.

[26] **Acknowledgments.** We thank Y. I. Stozhkov, O. S. Maksumov, A. N. Kvashnin and S. V. Mizin (project participants from Solar and Cosmic Ray Physics Laboratory of LPI RAS) for their interest and help. J.P.R., E.E. and R.R.S.M. thank CNPq and FAPESP agencies (Proc. 305655/2010-8, 301233/2011-0 and 2009/11935-5 respectively). Also, we would like to thank the NASA and the GATS Inc. for providing the SABER's data.

References

- Adamson, P., et al. (2010), Observation of muon intensity variations by season with the MINOS far detector. *Phys. Rev., D*(81), 012001, doi:10.1103/PhysRevD.81.012001.
- Ambrosio, M., et al. (1997), Seasonal variations in the underground muon intensity as seen by MACRO, *Astroparticle Phys.*, 7(1–2), 109–124, doi:10.1016/S0927-6505(97)00011-X.
- Berkova, M. D., A. V. Belov, E. A. Eroshenko, D. Smirnov, and V. G. Yanke (2008), Temperature effect of muon component and practical questions of its account, in *Proc. 21st European Cosmic Ray Symposium*, edited by P. Kiraly et al., pp. 123–126, Institute of Experimental Physics, Slovak Academy of Sciences, Kosice, Slovakia.
- Berkova, M. D., A. V. Belov, E. A. Eroshenko, and V. G. Yanke (2011), Temperature effect of the muon component and practical questions for considering it in real time, *Bull. Russ. Acad. Sci. Phys.*, 75(6), 820–824, doi:10.3103/S1062873811060086.
- Blackett, P. M. S. (1938) On the instability of the barytron and the temperature effect of cosmic rays, *Phys. Rev.*, 54(11), 973–974, doi:10.1103/PhysRev.54.973.
- De Mendonça, R. R. S., J.-P. Raulin, F. C. P. Bertoni, E. Echer, V. S. Makhmutov, and G. Fernandez (2011), Long-term and transient time variation of cosmic ray fluxes detected in Argentina by CARPET cosmic ray detector, *J. Atmos. Sol.-Terr. Phys.*, 73, 1410–1416, doi:10.1016/j.jastp.2010.09.034.
- Dorman, L. I. (1972), *The Meteorological Effects of Cosmic Rays*, Nauka Press, Moscow, Russia.
- Dorman, L. I. (2004), *Cosmic Rays in the Earth's Atmosphere and Underground*, Kluwer, Dordrecht, Netherlands.
- Duperier, A. (1949), The meson intensity at the surface of the earth and the temperature at the production level, *Proc. Phys. Soc. A*, 62(11), 684–696, doi:10.1088/0370-1298/62/11/302.
- French, W. R., and R. L. Chasson (1959), Atmospheric effects on the hard component of cosmic radiation near sea level, *J. Atmos. Terr. Phys.*, 14(1–2), 1–18, doi:10.1016/0021-9169(59)90051-0.
- Hayakawa, S., K. Ito, and Y. Terashima (1955), Positive temperature effect of cosmic rays, *Prog. Theor. Phys.*, 14(6), 497–510, doi:10.1143/PTP.14.497.
- Hess, V. F. (1940), On the seasonal and the atmospheric temperature effect in cosmic radiation, *Phys. Rev.*, 57(9), 781–785, doi:10.1103/PhysRev.57.781.
- Maeda, K., and M. Wada (1954), Atmospheric temperature effect upon cosmic ray intensity at sea level, *J. Sci. Res. Ins. (Tokyo)*, 48, 71–79.
- Mathews, P. M. (1959), Atmospheric effects on cosmic ray intensity at sea level, *Can. J. Phys.*, 37(2), 85–101, doi:10.1139/p59-015.
- Myssowsky, L., and L. Tuwim (1926), Unregelmässige Intensitätsschwankungen der Hohenstrahlung in geringer Seeöhe, *Zeitschrift für Physik A Hadrons and Nuclei*, 39(2–3), 146–150, doi:10.1007/BF01394307.
- Sagisaka, S. (1986), Atmospheric effects on cosmic-ray muon intensities at deep underground depths, *Il Nuovo Cimento C*, 9(4), doi:10.1007/BF02558081.
- Steinke, E. (1929), Wasserversenk-messungen der durchdringenden Hessschen Strahlung, *Zeitschrift für Physik A Hadrons and Nuclei*, 58(3–4), 183–193, doi:10.1007/BF01339040.
- Trefall, H. (1957), On the positive temperature effect in the cosmic radiation and the $\pi - \mu$ decay, *Physica*, 23(1-5), 65–72, doi:10.1016/S0031-8914(57)90472-X.
- Yanke, V. G., A. Asipenka, M. Berkova, R. R. S. de Mendonca, J.-P. Raulin, F. C. P. Bertoni, E. Echer, G. Fernández, and V. Makhmutov (2011), Temperature effect of general component seen by cosmic ray detectors, in *Proceedings of 32nd International Cosmic Ray Conference*, 11, 377–380.
- Yanchukovsky, V. L., G. Ya. Filimonov, and R. Z. Hisamov (2007), Atmospheric variations in muon intensity for different zenith angles, *Bull. Russ. Acad. Sci. Phys.*, 71(7), 1038–1040, doi:10.3103/S106287380707043X.
- Wang, C. P., and A. H. Lee (1967), Cosmic-ray muons and atmospheric coefficients near to geomagnetic equator, *J. Geophys. Res.*, 72(23), 6107–6109, doi:10.1029/JZ072i023p06107.
- Webber, W. R., and J. A. Lockwood (1988), Characteristics of the 22-year modulation of cosmic rays as seen by neutron monitors, *J. Geophys. Res.*, 93(A8), 8735–8740, doi:10.1029/JA093iA08p08735.